# A New Temperature Compensation Method by Optimizing the Structure of Extrinsic Fabry-Perot Interferometric Optical Fiber Sensor

Zhao Ziwen Wang Weiyu Zhang Min Xie Shangran LiaoYanbiao

(*Department of Electronic Engineering, Tsinghua University, Beijing* 100084, *China*)

**Abstract** For the problem of the change of capillary tube induced by thermal expansion and contraction with temperature change, a new temperature compensation method applied in extrinsic Fabry-Perot interferometric (EFPI) optical fiber sensor is proposed. Temperature compensation film (copper film in this paper) is deposited on the reflective fiber within silica tube to compensate the gap change caused by temperature variation. The experimental results prove the effectiveness of this method and a linear relationship between axial length of copper film and temperature compensation length is found. In experiment, the temperature compensation coefficient of 1 mm axial length copper film reaches 0.49 nm/℃.

**Key words** fiber optics; sensor; temperature compensation; temperature compensation film; extrinsic Fabry-Perot interferometric optical fiber sensor

**OCIS codes** 060.2300; 060.2310; 060.2370; 310.4925

# 通过改进非本征法布里-珀罗干涉型光纤传感器结构实现温度补偿的新方法

赵子文 王为宇 张 敏* 谢尚然 廖延彪

(清华大学电子工程系，北京 100084)

**摘要** 针对非本征法布里-珀罗干涉型(EFPI)光纤传感器外毛细管热胀冷缩引起的温度敏感问题，提出了通过在毛细管内部反射光纤表面镀温度补偿膜(实验中使用铜膜)来降低温度影响的方法，并推导了相关的数学模型，进行了实验研究。实验结果证明了该温度补偿方法的有效性和可控性。实验中，铜膜的轴向长度和补偿系数表现出了良好的线性关系，1 mm 轴向长度的铜膜温度补偿系数达到了 0.49 nm/℃。

**关键词** 光纤光学；传感器；温度补偿；温度补偿膜；非本征法布里-珀罗干涉型光纤传感器

**中图分类号** TN253 **文献标识码** A **doi**：10.3788/LOP50.090605

## 1 Introduction

Optical fiber sensors have numerous applications in manyfileds[1-6] due to their good durability, high precision, small size and insensitivity to electrical magnetic interference. As a type of optical fiber sensor, extrinsic Fabry-Perot interferometric (EFPI) optical fiber sensor can be easily fabricated and has good durability because of its use of a capillary of glass tube[7]; it can be used in measurements of strain, hydrogen concentration and so on[8-12].

But in the application of traditional EFPI optical fiber sensor constructed with capillary tube and optical fiber, in addition to the parameter to be measured, the sensor can be affected by other factors such as environment temperature. Different areas of measurement need different capillary tubes. Some capillary tubes have large temperature coefficient. The change of silica tube induced by thermal expansion and contraction with temperature change can thus affect the measurement seriously, whereas the temperature compensation methods are seldom reported, although it is necessary for further exploiting EFPI optical fiber sensor. The traditional method is to put a

**收稿日期**：2013-04-22；**收到修改稿日期**：2013-04-24；**网络出版日期**：2013-08-05

**基金项目**：国家自然科学基金(10776016)

**作者简介**：赵子文(1981—)，男，博士研究生，主要从事光纤传感方面的研究。E-mail：z_zwen@163.com

**导师简介**：廖延彪(1935—)，男，教授，主要从事光纤传感方面的研究。E-mail：lyb-dee@tsinghua.edu.cn

* **通信联系人**。E-mail：minzhang@mail.tsinghua.edu.cn

temperature sensor in measurement environment and then subtract the effects of temperature change by software. But it increases the complexity of system. In this paper, a new temperature compensation method by optimizing the structure of sensor is proposed, which uses a temperature compensation film. Experimental results prove the effectiveness of this method.

## 2 Sensor fabrication and temperature compensation principle

The improved structure and basic structure of EFPI sensor are shown in Fig. 1. Compared with the basic structure, metal film with a high temperature coefficient acting as the temperature compensation film is deposited on the reflective fiber surface of the improved structure. When temperature changes, the reflective fiber would experience an axial strain induced by temperature compensation film. It can reduce the effect of environment temperature variation on the gap length of EFPI sensor.

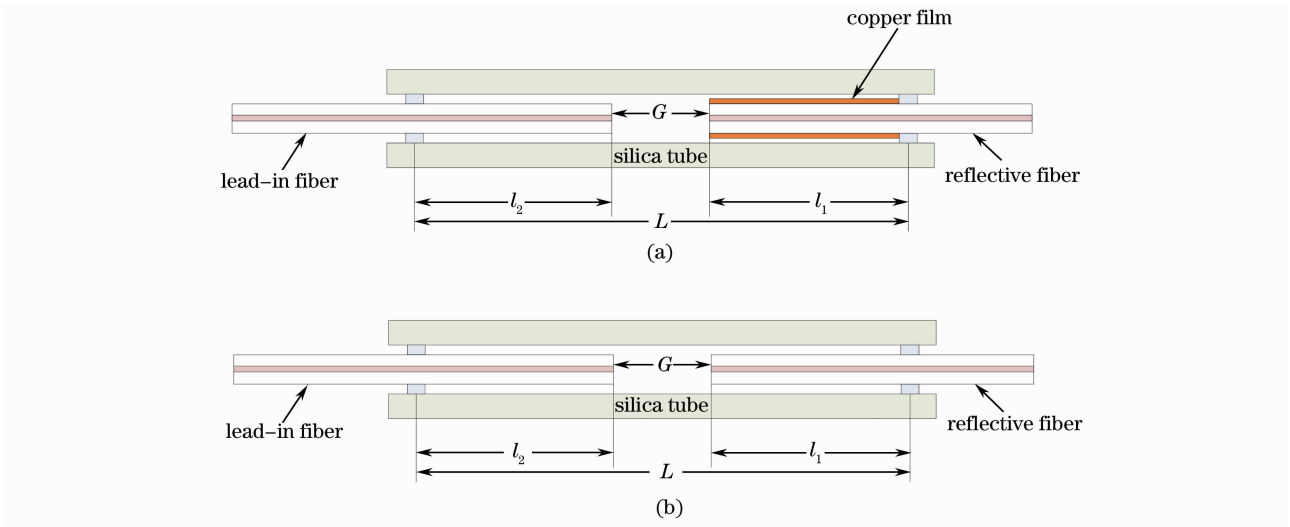


Fig. 1 Schematic of (a) the improved structure and (b) the basic structure of EFPI sensor

Because some parameters of compensationfilm are unknown, we cannot calculate the compensation results by mathematical model. The mathematical model is established only for proving the feasibility of this method. $L$ is the length of silica tube, $l_1$ and $l_2$ are lengths of reflective fiber in silica tube and length of lead-in fiber in silica tube, respectively (as shown in Fig. 1). $T_0$ is room temperature, and $T$ is measurement temperature.

Under the room temperature $T_0$, the length of the silica tube can be written as

$$L_0 = G_0 + (l_{10} + l_{20}). \tag{1}$$

When temperature changes $\Delta T$,

$$L = L_0 + \alpha_s \Delta T L_0 = L_0(1 + \alpha_s \Delta T), \tag{2}$$

$$l_2 = l_{20}(1 + \alpha_f \Delta T), \tag{3}$$

where $\alpha_s$ is the coefficient of thermal expansion of silica tube, $\alpha_f$ is the coefficient of thermal expansion of fiber, and $\Delta T = T - T_0$. If not stretched by compensation film, when temperature changes $\Delta T$, the length of reflective fiber in silica tube is $l'_{1f}$:

$$l'_{1f} = l_{10f} + \alpha_f \Delta T l_{10f} = l_{10f}(1 + \alpha_f \Delta T), \tag{4}$$

where $l_{10f}$ is the length of reflective fiber in silica tube at $T_0$. Now, we consider the axial force of the optical fiber stretched by compensation film deposited on reflective fiber, this axial force is $F$,

$$\frac{F}{S_f} = Y_f \cdot \frac{\Delta l_{1f}}{l'_{1f}}, \tag{5}$$

where $S_f$ is the cross-sectional area of fiber, $Y_f$ is the Young's modulus of fiber, $\Delta l_{1f} = l_{1f} - l'_{1f}$, $l_{1f}$ is the length of reflective fiber in silica tube after considering the compensation effect of compensation film. From Eq. (5),

$$F = S_f \cdot Y_f \cdot \frac{\Delta l_{1f}}{l'_{1f}}. \tag{6}$$

For the compensation film, if not stretched by fiber, when temperature changes $\Delta T$, with the definition that the axial length of compensation film deposited on the reflective fiber in silica tube is $l'_{1c}$, $\alpha_c$ is the coefficient of thermal expansion of compensation film, then

$$l'_{1c} = l_{10}(1 + \alpha_c \cdot \Delta T). \tag{7}$$

Now, we consider the axial force of the compensation film deposited on reflective fiber stretched by the reflective fiber. The axial force stretched by fiber is $-F$:

$$-F = S_c \cdot Y_c \cdot \frac{\Delta l_{1c}}{l'_{1c}}, \tag{8}$$

where $S_c$ is the cross-sectional area of compensation film, $Y_c$ the is Young's modulus of compensation film, $\Delta l_{1c} = l_{1c} - l'_{1c}$, $l_{1c}$ is the axial length of compensation film deposited on reflective fiber in silica tube after considering the axial force stretched by fiber.

From Eqs.(6) and (8), we can get

$$S_f Y_f \cdot \frac{\Delta l_{1f}}{l'_{1f}} = -S_c Y_c \cdot \frac{\Delta l_{1c}}{l'_{1c}}, \tag{9}$$

Equations(4), (7), and $\Delta l_{1f} = l_{1f} - l'_{1f}$, $\Delta l_{1c} = l_{1c} - l'_{1c}$ are brought into this equation (we use $l_{1f} = l_{1c} = l_1$), so that we get

$$l_1 = \frac{S_f Y_f + S_c Y_c}{\dfrac{S_f Y_f}{1 + \alpha_f \Delta T} + \dfrac{S_c Y_c}{1 + \alpha_c \Delta T}} \cdot l_{10}. \tag{10}$$

Setting $x_{\Delta T} = \dfrac{S_f Y_f + S_c Y_c}{\dfrac{S_f Y_f}{1 + \alpha_f \Delta T} + \dfrac{S_c Y_c}{1 + \alpha_c \Delta T}}$, we get

$$l_1 = x_{\Delta T} \cdot l_{10}. \tag{11}$$

The gap length is

$$G = L - (l_1 + l_2).$$

Equations(1)~(3) and (11), are brought into the above equation, and then the gap length can be obtained by

$$G = G_0(1 + \alpha_s \cdot \Delta T) + l_{10}(1 + \alpha_s \Delta T - x_{\Delta T}) + l_{20}(\alpha_s - \alpha_f)\Delta T. \tag{12}$$

The change of gap length caused by temperature change is written as

$$\Delta G = G - G_0 = G_0 \alpha_s \cdot \Delta T + l_{10}(1 + \alpha_s \Delta T - x_{\Delta T}) + l_{20}(\alpha_s - \alpha_f)\Delta T. \tag{13}$$

## 3 Experiment and discussion

The basic structure of our EFPI sensor is shown in Fig.1. The lead-in fiber and reflective fiber were welded at both ends of the silica tube with $CO_2$ laser. The axial distance between two fixed points was 47 mm. The diameters of lead-in fiber and reflective fiber were both 125 μm. The outer and inner diameters of the silica tube were 300 μm and 130 μm, respectively. The length of silica tube was 50 mm. The optical fiber model was Corning SMF-28.

Firstly, the temperature coefficient of the sensor without temperature compensation film was investigated. The temperature measurement system is shown in Fig.2. The EFPI sensor was illuminated by a LED source (Honeywell HEF4222) around 850 nm through a 2×2 coupler. The interferential light returned from an HR2000+ spectrometer from Ocean Optics, which provided an optical resolution as good as 0.035 nm, and the spectrometer was connected to a personal computer via USB port to analyze the store data. The cross-correlation signal processing method was used to calculate the change of gap length as our previous work[12]. In temperature experiment, the samples were placed in a programmable temperature and humidity chamber (TYH-1P Gaoyu Technical Co., Ltd.) where both temperature and humidity can be controlled precisely. The relative humidity of measurement environment was set to

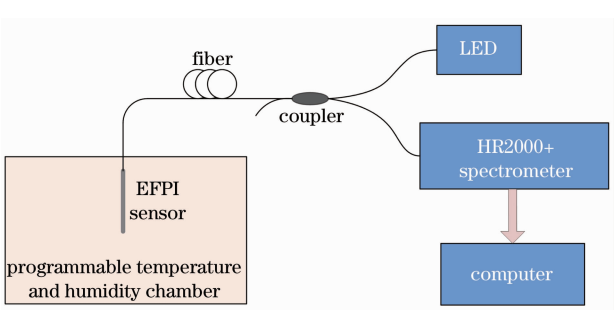


Fig.2 Schematic of experimental setup

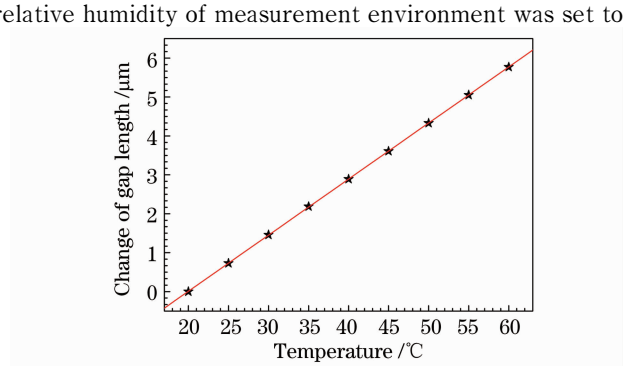


Fig.3 Temperature characteristics of the EFPI sensor without compensation film

50%. Temperature was warmed up from 20 ℃ to 60 ℃, recorded every 5 ℃. The results are shown in Fig. 3. It can be seen that the temperature coefficient of sensor without temperature compensation film reaches 144.3 nm/℃.

Temperature compensation experiments were carried out. In this report, we chose copper as the temperature compensation film because copper has relatively higher temperature coefficient and lower price. In temperature compensation experiment, a copper film with thickness of approximately 1 μm was deposited on the surface of reflection fiber by magnetron sputtering. For the reason of enhancing adhesion between copper film and optical fiber, the titanium film about 10 nm was deposited on optical fiber as a buffer layer before depositing copper film. The cross section of the copper temperature compensation film deposited on reflective fiber was observed by scanning electron microscopy (SEM), as shown in Fig. 4. Figure 4(a) is an overall cross section of fiber deposited copper film, and Figs. 4(b)～(d) are 3 different positions of the junction of fiber surface and copper film. These images show that the copper film has a relative uniform thickness. We prepared 6 samples, in which the axial lengths of the copper film are 0, 8.5, 13.5, 19.5, 23 and 35 mm, respectively. At room temperature, the gap lengths of all the EFPI sensors are between 50 μm and 80 μm. Compared with the length of silica tube, lead-in fiber and reflective fiber, the value of gap length is so small that the effect of the different gap lengths on the experiment results could be ignored in this experiment. Experiment results are listed in Table 1 and shown in Fig. 5.

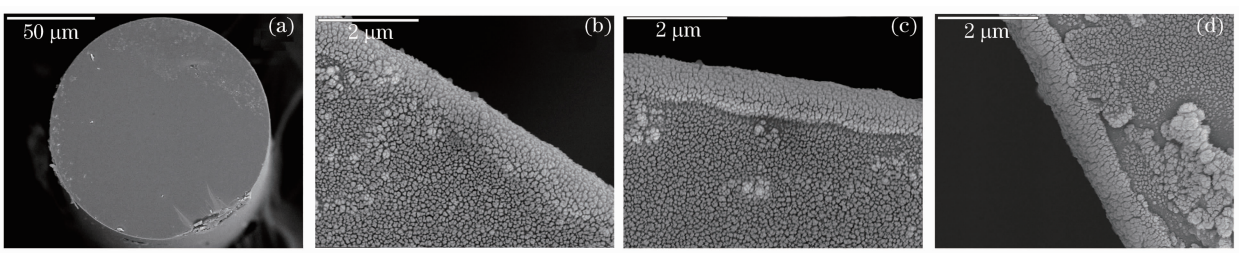


Fig. 4 SEM images of the cross section of copper temperature compensation film deposited on reflective fiber. (a) Overall cross section of fiber deposited copper film; (b)～(d) 3 different positions of the junction between fiber surface and copper film

Table 1 Temperature compensation results of different axial lengths of copper film

| Copper length /mm | 0 | 8.5 | 13.5 | 19.5 | 23 | 35 |
|---|---|---|---|---|---|---|
| Temperature coefficient of sensors (nm/℃) | 144.3 | 141.0 | 137.4 | 135.8 | 134.0 | 127.0 |
| Temperature compensation coefficient (nm/℃) | 0 | 3.3 | 6.9 | 8.5 | 10.3 | 17.3 |

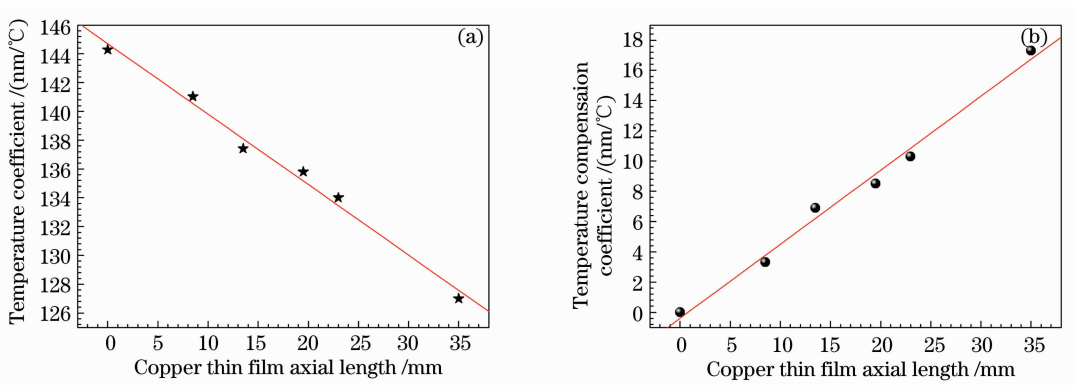


Fig. 5 Temperature compensation results of different axial length of copper film. (a) Temperature coefficient of sensors; (b) temperature compensation coefficient

For the sensor without temperature compensation copper film, the temperature coefficient of sensor was 144.3 nm/℃. The temperature coefficient of sensor was decreased with the increasing of axial length of copper film. For the sample with a temperature compensation copper film of 35 mm axial length, the temperature coefficient of sensor decreased to 127.0 nm/℃, and the temperature compensation coefficient of the copper film reached 17.3 nm/℃. From Fig. 5, we can see a linear relationship between axial length of copper film and temperature compensation coefficient. In this experiment, the temperature compensation coefficient of 1 mm axial length copper reached 0.49 nm/℃. Experimental results proved that this temperature compensation method was effective and the temperature compensation coefficient could be controlled by choosing the suitable axial length of copper film. The

silica tubes chosen in this paper have larger temperature coefficient. If we choose the silica tube with suitable temperature coefficient in the range of temperature compensation of copper film, this temperature compensation method can completely eliminate the influence of measurement environment temperature change.

## 4 Conclusion

In summary, a new temperature compensation method by deposited copper film on reflective optical fiber of EFPI sensor was proposed and its mathematical model was established. Experimental results proved that this method was effective, and under our experiment condition, the temperature compensation coefficient of 1 mm axial length copper reached 0.49 nm/℃. Further investigations on temperature compensation film are in progress, including depositing thicker copper films, improving the crystal quality of copper film and choosing more suitable material as temperature compensation film. We believe that the performance of temperature compensation film will be further improved with the development of our investigations.

## References


1 Y C Yang, K S Han. Damage monitoring and impact detection using optical fiber vibration sensors [J]. Smart Mater Struct, 2002, 11(3): 337 - 345.

2 Wang Wenyuan, Wen Jianxiang, Pang Fufei, *et al*.. All single-mode fiber Fabry-Perot interferometric high temperature sensor fabricated with femtosecond laser [J]. Chinese J Lasers, 2012, 39(10): 1005001.
王文辕, 文建湘, 庞拂飞, 等. 飞秒激光制备的全单模光纤法布里-珀罗干涉高温传感器[J]. 中国激光, 2012, 39(10): 1005001.

3 Yao Jun, Zhu Tao, Deng Ming, *et al*.. A humidity sensor based on all-fiber Fabry-Perot interferometer formed by large offset splicing [J]. Chinese J Lasers, 2012, 39(s1): s114004.
姚 军, 朱 涛, 邓 明, 等. 基于大偏置熔接的全光纤法布里-珀罗湿度传感器[J]. 中国激光, 2012, 39(s1): s114004.

4 Xia Juan, Sui Chenghua, Liu Yuling, *et al*.. Reflective optical fiber temperature sensor based on temperature-dependent optical properties of ZnO film [J]. Chinese J Lasers, 2011, 38(2): 0205003.
夏 娟, 隋成华, 刘玉玲, 等. 基于 ZnO 薄膜光学温变特性的反射式光纤温度传感器[J]. 中国激光, 2011, 38(2): 0205003.

5 Zhu Ji, Later Khalil, Zhang Jianzhong, *et al*.. Lquid-solid phase transition monitoring based on FBG [J]. Laser & Optoelectronics Progress, 2012, 49(1): 010601.
竺 绩, Later Khalil, 张建中, 等. 基于光纤光栅的液固相变监测[J]. 激光与光电子学进展, 2012, 49(1): 010601.

6 Chen Yixin, Zhao Chunliu, Liu Xing, *et al*.. Research and development of optical fiber sensors based on photonic crystal fiber loop mirrors [J]. Laser & Optoelectronics Progress, 2012, 49(1): 010005.
陈益新, 赵春柳, 刘 星, 等. 基于光子晶体光纤环镜的光纤传感器的研究及进展[J]. 激光与光电子学进展, 2012, 49(1): 010005.

7 Sang-Hoon Kim, Jung-Ju Lee, Dong-Soo Kwon. Signal processing algorithm for transmission-type Fabry-Perot interferometric optical fiber sensor [J]. Smart Mater Struct, 2001, 10(4): 736 - 742.

8 Ying Huang, Tao Wei, Zhi Zhou, *et al*.. An extrinsic Fabry-Perot interferometer-based large strain sensor with high resolution [J]. Measurement Science and Technology, 2010, 21(10): 105308.

9 Dae-Cheol Seo, Jung-Ju Lee, Il-Bum Kwon. Monitoring of fatigue crack growth of cracked thick aluminum plate repaired with a bonded composite patch using transmission-type extrinsic Fabry-Perot interferometric optical fiber sensors [J]. Smart Mater Struct, 2002, 11(6): 917 - 924.

10 T Liu, M Wu, Y Rao, *et al*.. A multiplexed optical fibre-based extrinsic Fabry-Perot sensor system for *in-situ* strain monitoring in composites [J]. Smart Mater Struct, 1998, 7(4): 550 - 556.

11 J S Zeakes, K A Murphy, A Elshabini-Raid, *et al*.. Modified extrinsic Fabry-Perot interferometric hydrogen gas sensor [C]. Proceedings of the Institute of Electrical and Electronics Engineers Lasers and Electro-Optics Society Annual Meeting, IEEE, 1994, 2: 235 - 236.

12 Z Yang, M Zhang, Y B Liao, *et al*.. Extrinsic Fabry-Perot interferometric optical fiber hydrogen detection system [J]. Appl Opt, 2010, 49(15): 2736 - 2740.